Imidazole Functionalized Magnesium Phthalocyanine Photosensitizer: Modified Photophysics, Singlet Oxygen Generation and Photooxidation Mechanism

ARTICLE *in* THE JOURNAL OF PHYSICAL CHEMISTRY A · JUNE 2012

Impact Factor: 2.69 · DOI: 10.1021/jp3047938 · Source: PubMed

THE JOURNAL OF PHYSICAL CHEMISTRY A

Article

pubs.acs.org/JPCA

Imidazole Functionalized Magnesium Phthalocyanine Photosensitizer: Modified Photophysics, Singlet Oxygen Generation and Photooxidation Mechanism

Xian-Fu Zhang*[,†,‡] and Wenfeng Guo[†]

[†]Chemistry Department & Center of Instrumental Analysis, Hebei Normal University of Science and Technology, Qinhuangdao, Hebei Province, 066004 China

[‡]MPC Technologies, Hamilton, Ontario, Canada L8S 3H4

ABSTRACT: Magnesium phthalocyanine (MgPc) was covalently attached by four imidazole units to form a novel photosensitizer (PS). The photophysical processes within the dyad PS were explored by steady state and time-resolved fluorescence as well as laser flash photolysis. Although the imidazole units caused a 50% decrease in fluorescence quantum yield and a remarkable shortening of fluorescence lifetime of the MgPc moiety, the triplet yield (Φ_T) is higher and the triplet lifetime becomes longer. The transient absorption bands for $MgPc^{\bullet-}$ were observed, indicating the occurrence of intramolecular photoinduced electron transfer (PET) from imidazole subunits to the lowest excited singlet state (S_1) of the MgPc moiety. The kinetic and thermodynamic analysis also supports the involvement of PET in S_1 deactivation. The quantum efficiency of photosensitized oxidation of diphenylisobenzofuran (DPBF) by the PS is 0.52. This value is much higher than Φ_T (0.26), since DPBF is photo-oxidized not only by singlet oxygen (type II reaction, 54%) but also by superoxide anion radical (type I reaction, 46%). The result suggests that the mechanism of photosensitized oxidation could be changed upon the conjugation of a PS to biological molecules, so that the importance of type I reaction is enhanced.

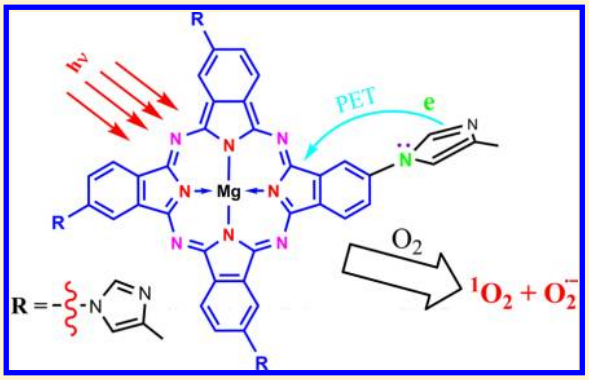

INTRODUCTION

Traditional cancer therapies, such as surgery, radiotherapy, and chemotherapy, suffer from the lack of selectivity in removing and destroying tumor tissues. Photodynamic therapy of tumor (PDT) is under intensive development to address the issue.[1−3] Phthalocyanine (Figure 1) is a type of often used photosensitizer (PS) in PDT.[4−7] The excited state interaction of PS with biomolecules plays a key role to understand the mechanism for PDT and design the new generation PS.[3] There are two types of mechanisms in PDT: type I, due to photoinduced electron transfer (PET) between PS excited states and biomolecules to produce active free radicals, and type II, caused by energy transfer from triplet state of a PS to molecular oxygen to generate reactive singlet oxygen.[8]

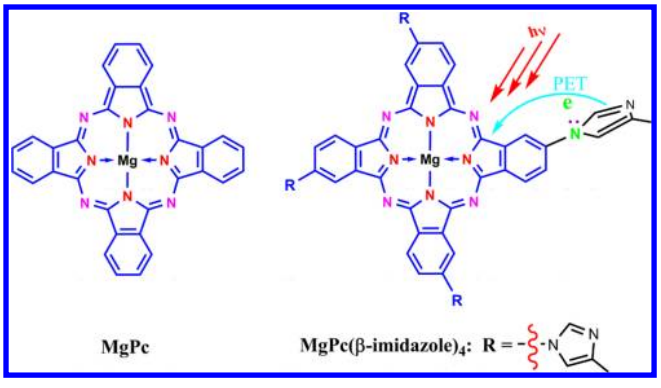

Figure 1. Chemical Structure of MgPc(β-imidazole)$_4$.

In practice, a working PS molecule is localized within solid tumor tissues, which causes difficulty in mechanism study. Therefore a lot of investigations on PDT mechanism have been carried out in aqueous solution, in which amino acids were employed as substrates for photosensitized electron transfer or singlet oxygen quenching.[9−14] The mechanism in aqueous solution is probably quite different from that in the solid tumor, since a PS molecule is adsorbed on tissues and directly contacts various aromatic electron donor moieties, such as N-containing amino acid residues. Hence the interaction is more similar to that of the intramolecular electron donor−acceptor case (interaction through bonding). The intermolecular photoinduced electron transfer (PET) between phthalocyanine PS and amino acid donors has been evidenced previously.[9−14]

A PS linked with biomolecules can be considered as intramolecular electron donor−acceptor (D−A) pairs, which usually make PET or energy transfer process from S_1 (lowest excited singlet state) of PS much faster than that of

Received: May 17, 2012
Revised: June 10, 2012
Published: June 19, 2012

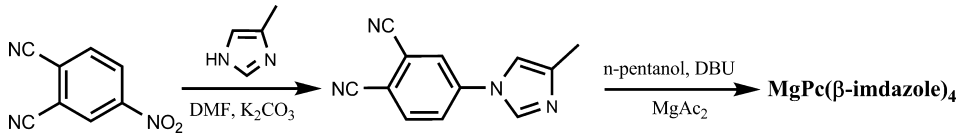

Figure 2. Synthetic path for MgPc(β-imidazole)$_4$.

intermolecular cases. Proteins or peptides contain up to 23 amino acid residues, all of which could act as electron donors which make the clear elucidation of photo events within protein/peptide conjugated PS difficult. Tryptophan, histidine, and tyrosine, however, are generally considered as the most active components in protein for PDT. To simplify the problem, imidazole, the main reactive component in histidine, was selected and attached to magnesium phthalocyanine (MgPc) in this study (Figure 1). Phthalocyanines were selected since they have been tested both in vitro[12,15−24] and in vivo[25,26] to be effective photosensitizers for PDT. We show in this report that the imidazole modification of MgPc significantly changes the mechanism of photosensitized oxidation while still maintaining the photosensitizing ability.

EXPERIMENTAL SECTION

Reagents and Apparatus. All reagents for synthesis were analytical grade and used as received. Dimethylformamide (DMF) was dried and redistilled before use. ^{1}H NMR spectra were recorded at room temperature on a Bruker dmx 300 MHz NMR spectrometer. MS spectra were recorded either on a Bruker APEX II or on an Autoflex III MALDI-TOF spectrometer. IR spectra were recorded at room temperature on a Shimadzu FTIR-8900 spectrometer. UV−visible spectra were recorded on a Shimadzu 4500 spectrophotometer using 1 cm matched quartz cuvettes.

Synthesis of 4-(4-Methyl-1*H*-imidazol-1-yl)-phthalonitrile. 1.73 g (0.01 mol) of 4-nitrophthalonitrile and 0.82 g (0.01 mol) of 4-methylimidazole were added to 20 mL of DMF in argon atmosphere, and the resulting solution was stirred at room temperature under argon for 48 h, during which 4.1 g (0.03 mol) of anhydrous potassium carbonate was added in four equal portions every two hours. The product solution was then poured into 100 mL of ice−water to precipitate, and the filtered solid was washed with water neutral pH and dried under vacuum. White needle (0.37 g) was obtained after recrystallization with hexane−ethanol solvent. Yield: 18%. Mp 200−201 °C. IR(KBr), ν(cm^{-1}): 3115, 3005, 1606, 1520, 1400 (Ar−H), 2235 (C≡N), 1070 (Ar−N). ^{1}H NMR (CDCl$_3$, ppm): δ 8.05−8.09 (d, 1H), 7.95−7.99 (d, 1H), 7.78−7.83 (s, 1H), 7.42−7.52 (s, 1H), 7.13−7.16 (s, 1H), 2.21−2.32 (s, 3H). MS, m/z: 208 [M − 1]$^-$.

Synthesis of Tetra[β-4-methyl-1*H*-imidazol-1-yl] MgPc, MgPc(β-imidazole)$_4$. The two-step procedure for the synthesis of MgPc(β-imidazole)$_4$ is shown in Figure 2. It is a well-established procedure which has been extensively discussed in the literature.[27]

Magnesium acetate (0.040 g, 0.18 mmol), 4-(4-methyl-1*H*-imidazol-1-yl)phthalonitrile (0.15 g, 0.70 mmol), and 9 mL of dried *n*-pentanol were mixed and stirred at 135 °C for 4 h under argon atmosphere in the presence of two drops of DBU as catalyst. After cooling down, the green precipitate was collected by filtration and washed with *n*-pentanol and *n*-hexane. The dried crude product was dissolved in THF and purified by column chromatography (silica gel) using THF as the mobile phase. Yield: 39%. UV−vis (DMF): λ_{max} nm (log ε) 360 (4.81), 618 (4.43), 682 (5.15). IR [(KBr) ν_{max}/cm^{-1}]: 3053 (Ar−H), 1608, 1519 (Ar C═C), 1490, 1332 (CH$_3$), 1137, 1049, 895 (N−Mg), 742. ^{1}H NMR (DMSO): δ, ppm 8.58−9.11 (4H, s, broad), 8.58 (4H, s), 7.93−8.31 (4H, s, broad), 7.92 (4H, s), 7.70−7.91(4H, s, broad), 2.39 (12H, s). Anal. ($C_{48}H_{32}N_{16}Mg$): C, 67.26 H, 3.76 N, 26.14; found C, 67.11 H, 3.96 N, 25.96. MALDI-TOF-MS, m/z: calculated 857.3; found 857.9 [M + 1]$^+$.

Photophysical Measurements. The absorption and fluorescence spectra, fluorescence quantum yields, and excited singlet state lifetimes, as well as triplet properties, were investigated at room temperature, ca. 22 °C. Steady state fluorescence spectra were acquired on a FLS 920 instrument. All spectra were corrected for the sensitivity of the photomultiplier tube. The fluorescence quantum yield (Φ_f) was measured by using

$$\Phi_f = \Phi_f^0 \cdot \frac{F_s}{F_0} \cdot \frac{A_0}{A_s} \frac{{n_s}^2}{{n_0}^2} \quad (1)$$

in which F is the integrated fluorescence intensity, A is the absorbance at excitation wavelength, n is the refractive index of the solvent used, the subscript 0 stands for a reference compound, and s represents samples. MgPc was used as the reference (Φ_f^0 = 0.30).[28,29] Excitation wavelengths of 610 nm corresponding to the vibronic band of S_0 to S_1 transitions were employed. The sample and reference solutions were prepared with the same absorbance (A_i) at the excitation wavelength (near 0.09 per cm) in the same solvent DMF. All solutions were air saturated for Φ_f measurements.

The fluorescence lifetime of S_1 was measured by the time-correlated single photon counting method (Edinburgh FLS920 spectrophotometer) with excitation at 672 nm diode laser (50 ps fwhm), and emission was monitored at 690 and 730 nm.

Transient absorption spectra were recorded in degassed DMF (prepared by bubbling with argon for 20 min) with an Edinburgh LP920 laser flash photolysis system. A Nd:YAG laser (Brio, 355 nm and 4 ns fwhm) was used as excitation source. The analyzing light was from a pulsed xenon lamp. The laser and analyzing light beams perpendicularly passed through a quartz cell with an optical path length of 1 cm. The signal was displayed and recorded on a Tektronix TDS 3012B oscilloscope and an R928B detector. The laser energy incident at the sample was attenuated to ca. 20 mJ per pulse. Time profiles at a series of wavelengths from which point-by-point spectra were assembled were recorded with the aid of a Pc controlled kinetic absorption spectrometer. The concentrations of the target compounds were typically 15 μM providing A_{355} = 0.40 in a 10 mm cuvette.

The triplet−triplet absorption coefficients ($\Delta\varepsilon_T$) of the samples were obtained using the singlet depletion method,[30] and the following equation was used to calculate the $\Delta\varepsilon_T$.

$$\Delta\varepsilon_T = \varepsilon_S \frac{\Delta A_T}{\Delta A_S} \quad (2)$$

dx.doi.org/10.1021/jp3047938 | J. Phys. Chem. A 2012, 116, 7651−7657

where ΔA_S and ΔA_T are the absorbance change of the triplet transient difference absorption spectrum at the minimum of the bleaching band and the maximum of the positive band, respectively, and ε_S is the ground state molar absorption coefficient at the UV−vis absorption band maximum. Both ΔA_S and ΔA_T were obtained from the triplet transient difference absorption spectra.

The triplet quantum yield Φ_T was obtained by comparing the ΔA_T of the optically matched sample solution at 355 nm in a 1 cm cuvette to that of the reference using the equation[30]

$$\Phi_T = \Phi_T^{ZnPc} \cdot \frac{\Delta A_T}{\Delta A_T^{ZnPc}} \cdot \frac{\Delta \varepsilon_T^{ZnPc}}{\Delta \varepsilon_T} \quad (3)$$

where the superscript represents the reference, ΔA_T is the absorbance of the triplet transient difference absorption spectrum at the selected wavelength, and $\Delta \varepsilon_T$ is the triplet state molar absorption coefficient.

Singlet oxygen quantum yield (Φ_Δ) determinations were carried out using the chemical trapping method.[31] Typically, a 3 mL portion of the respective PS solutions that contained diphenylisobenzofuran (DPBF) was irradiated at 660 nm in air saturated DMF. The Φ_Δ value was obtained by the relative method using MgPc as the reference (eq 4):

$$\Phi_\Delta = \Phi_\Delta^{ref} \frac{k}{k^{ref}} \frac{I_a^{ref}}{I_a} \quad (4)$$

where Φ_Δ^{ref} is the singlet oxygen quantum yield for the standard (0.60 for MgPc in DMF);[32] k and k^{ref} are the DPBF photobleaching rate constants in the presence of the respective samples and standard, respectively; and I_a and I_a^{ref} are the rates of light absorption at the irradiation wavelength of 660 nm by the samples and standard, respectively. Their ratio can be obtained by eq 5.

$$\frac{I_a^{ref}}{I_a} = \frac{1 - 10^{-A_{670}^{ref}}}{1 - 10^{-A_{670}}} \quad (5)$$

To avoid chain reactions induced by DPBF in the presence of singlet oxygen, the concentration of DPBF was lowered to ~3 × 10^{-5} mol dm^{-3}. A solution of sensitizer (absorbance ~0.70 at the irradiation wavelength) that contained DPBF was prepared in the dark and irradiated in the Q-band region. DPBF degradation was monitored by UV−vis absorption spectrum. The error in the determination of Φ_Δ was ~10% (determined from several Φ_Δ values).

RESULTS AND DISCUSSION

An imidazole unit in MgPc(β-imidazole)$_4$ is an independent aromatic system from the linked MgPc π-system. Its presence causes a 50% decrease of fluorescence quantum yield (Φ_f) and the shortening of fluorescence lifetime (τ_f) significantly from 7.49 to 5.85 ns. The τ_f decrease shows that the imidazole units interact with the lowest excited state (S_1) of MgPc through photoinduced electron transfer (PET) or energy transfer (PeT) within the donor−acceptor pair. In contrast to the suppression on fluorescence properties, the quantum yield of triplet formation (Φ_T) is slightly increased and the triplet lifetime (τ_T) becomes longer from 214 to 275 μs.

To understand the above observations, ground state and time-resolved absorption spectra were also measured to reveal the transient species involved, including triplet state (T_1) and $MgPc^{\bullet-}$ (Figures 3−5).

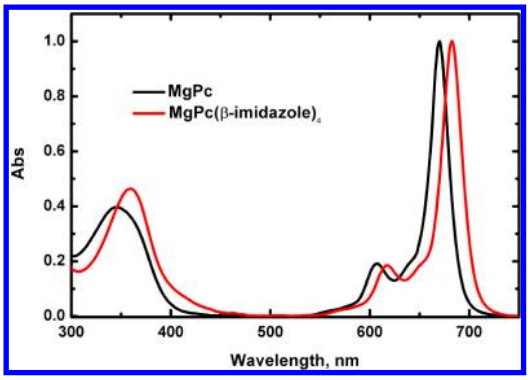

Figure 3. UV−vis absorption spectra of MgPc (5 μM) and MgPc(β-imidazole)$_4$ (7.1 μM) in DMF.

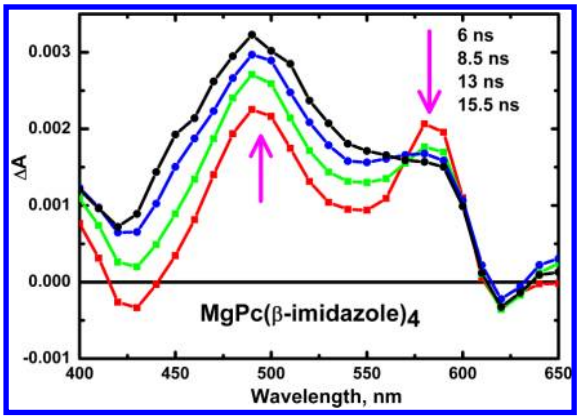

Figure 4. Nanosecond scaled transient absorption spectra of MgPc(β-imidazole)$_4$ in argon purged DMF, 15 μM, excitation wavelength 355 nm.

Ground State Absorption. The UV−vis absorption spectrum of MgPc(β-imidazole)$_4$ is compared with that of MgPc in Figure 3. The spectral shape of the two spectra is almost identical in the visible region, although a slight red shift in absorption maximum occurred upon the presence of imidazole units. This small red shift (12 nm) and the identical shape in absorption spectrum support that the imidazole is not π-conjugated with the MgPc aromatic ring.

Therefore the imidazole units and the MgPc moiety in MgPc(β-imidazole)$_4$ are mutually independent π-systems which form a donor−acceptor pair, in which an imidazole acts as the electron donor, and MgPc is the electron acceptor.

Nanosecond Transient Absorption Spectra (TAS). Figure 4 shows the evolution of the TAS of MgPc(β-imidazole)$_4$ during the first 16 nanoseconds. Absorption bands at 580 and 650 nm due to the anion radical of MgPc[33] ($MgPc^{\bullet-}$) are now clearly resolvable in additional to T_1−T_n absorption at 500 nm. The occurrence of $MgPc^{\bullet-}$ indicates the PET process from imidazole units to the MgPc moiety:

$$^1\text{MgPc–imidazole} \xrightarrow{\text{PET}} \text{MgPc}^{\bullet-}\text{–imidazole}^{\bullet+}$$

Also noted is that the decay of $MgPc^{\bullet-}$ at 580 nm is accompanied by the increase in T_1−T_n absorption at 500 nm, suggesting that the separated charge state (CSS) recombines to form the triplet state:

$$\text{MgPc}^{\bullet-}\text{–imidazole}^{\bullet+} \xrightarrow[\text{CR}]{} {}^3\text{MgPc–imidazole}$$

dx.doi.org/10.1021/jp3047938 | J. Phys. Chem. A 2012, 116, 7651−7657

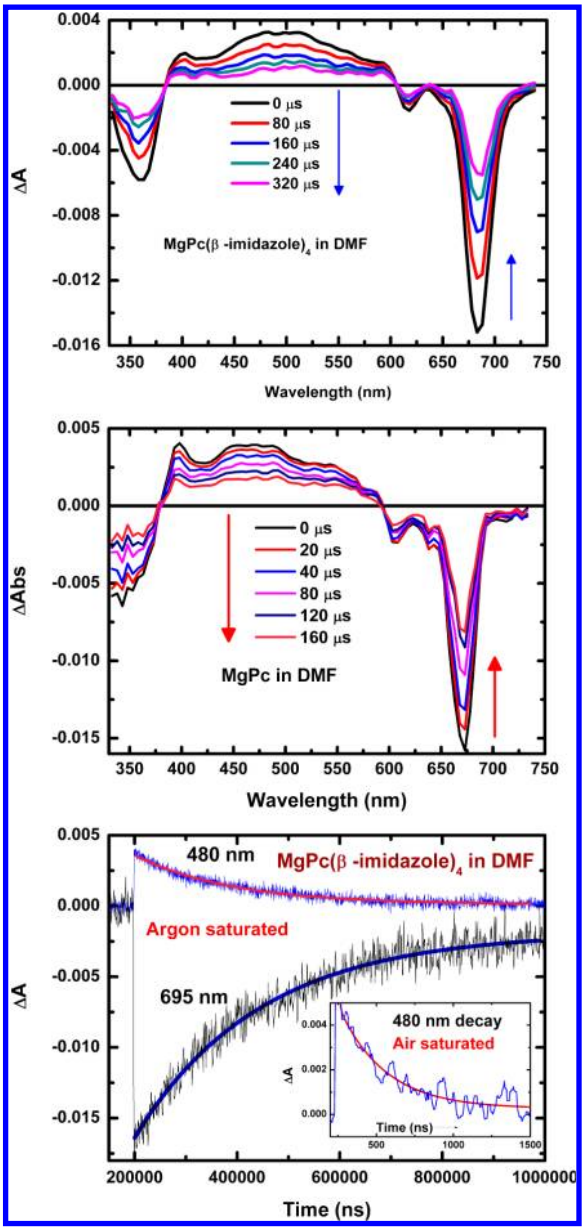

Figure 5. Top and middle: Microsecond scaled transient absorption spectra of MgPc(β-imidazole)$_4$ (top) and MgPc (middle) in argon purged DMF, 15 μM, excitation wavelength 355 nm. Bottom: Decay of positive transient signal and recovery of negative ground state absorption in argon saturated DMF for MgPc(β-imidazole)$_4$, excitation with 355 nm laser pulse. Inset is the decay at 480 nm in air saturated DMF.

In air saturated DMF solutions, the absorption bands at 580 and 650 nm were quenched, indicating that molecular oxygen can effectively react with $MgPc^{\bullet-}$ by capturing the electron: $MgPc^{\bullet-} + O_2 \rightarrow MgPc + O_2^{\bullet-}$. The formed $O_2^{\bullet-}$ can be trapped by DMPO and recorded by ESR, for which we have reported previously.[34]

Microsecond Scaled Transient Absorption Spectra. TAS in μs scale are compared in Figure 5 for MgPc(β-imidazole)$_4$ and MgPc. These spectra were recorded in argon saturated DMF with excitation at 355 nm by a 4 ns pulsed laser. TAS of MgPc (Figure 5 middle) is typical of triplet−triplet (T_1−T_n) absorptions for Pcs and in good agreement with that reported for Pc.[30] TAS of MgPc(β-imidazole)$_4$ (Figure 5 top) is similar to that of MgPc in spectral shape, but the absorption maximum is 25 nm red-shifted, and the bands are assigned to T_1−T_n absorption of MgPc(β-imidazole)$_4$ by analogy and also based on the following analysis.

The minimum of negative absorptions in the B- and Q-band region showed peaks matching the absorption maximum of the corresponding ground state absorption; the positive bands are separated from the ground state bleaching with well-defined isosbestic points, and the bleaching recovery is synchronous to the positive absorption decay, indicating concomitant behavior, i.e., as the positive T_1−T_n absorption decays, the ground state is repopulated. The transient decay at 480 nm is also given in Figure 5 for MgPc(β-imidazole)$_4$, and the concomitant bleaching recovery at ground state absorption minimum of 695 nm is also included. These curves can all be well fit by the monoexponential function.

The triplet lifetime (τ_T) thus obtained is collected in Table 1. The τ_T values are 214 μs for MgPc and 275 μs for MgPc(β-imidazole)$_4$, respectively. The result suggests that attached imidazole units do not quench T_1 of MgPc, i.e., no PET or PeT between imidazoles and T_1 of MgPc occurs. This is in contrast with the case of the S_1 state, from which PET does proceed. The τ_T values are comparable to those of other Pcs[35,36] and are all sufficiently long for photosensitizing the production of singlet oxygen.

In air saturated DMF solution, however, the τ_T of MgPc(β-imidazole)$_4$ is shortened dramatically to 0.30 μs (inset of Figure 5 bottom), while that of MgPc is reduced to 0.35 μs. The rate constant by oxygen quenching can be then evaluated to be 1.67×10^9 M^{-1} s^{-1} for MgPc(β-imidazole)$_4$ and 1.46×10^9 M^{-1} s^{-1} for MgPc, which are close to the diffusion rate constant. This effective oxygen quenching also suggests that the positive absorptions are due to T_1−T_n triplet absorptions. The triplet absorption coefficient ($\Delta\varepsilon_T$) was determined to be 29670 M^{-1} cm^{-1} for MgPc(β-imidazole)$_4$. The triplet formation quantum yield was measured to be 0.26, higher than 0.18 for MgPc.

In this microsecond time scale, no transient species other than T_1 was found from TAS in Figure 5. This also shows that no triplet quenching is present, and hence no PET originates from the T_1 state. Within this time range, $MgPc^{\bullet-}$−$imidazole^{\bullet+}$ due to PET from S_1 is not observable, because the CSS is generated and decayed within a few nanoseconds. Since the half of S_1 states of the MgPc moiety are not quenched by the conjugated imidazoles, ISC (intersystem crossing, i.e., process

Table 1. Photophysical Properties in DMF[a]

	λ_{max}^{abs}, nm	log ε	λ_{max}^{em}, nm	$\Delta\bar{\nu}$, cm^{-1}	E_s, eV	Φ_f	τ_f, ns	χ^2	λ_{max}^{T-T}, nm	$\Delta\varepsilon_T$, M^{-1} cm^{-1}	Φ_T	τ_T, μs	Φ_Δ	Φ_{PET}
MgPc	670	5.30	682	264.2	1.84	0.60	7.49	1.01	475	46000	0.18	214	0.48	n.a.
MgPc(β−imidazole)$_4$	682	5.15	693	230.1	1.81	0.31	5.85	1.02	500	29670	0.26	275	0.52	0.22

[a] λ_{max}^{abs} is the UV−vis absorption maximum. λ_{max}^{em} is the fluorescence emission maximum. $\Delta\bar{\nu}$ is the Stokes shift. E_s is the energy of lowest excited state (S_1). Φ_f is the fluorescence quantum yield. τ_f is the fluorescence lifetime. χ^2 is the chi squared value for the fitting of emission decay.

dx.doi.org/10.1021/jp3047938 | J. Phys. Chem. A 2012, 116, 7651−7657

ii) from S_1 can still effectively proceed, which will compete with process iii, i.e., S_1 quenching by imidazoles as below.

$$\text{absorption: MgPc}-\text{imidazole} \xrightarrow[\text{fs}]{h\nu} \text{MgPc}(S_1)-\text{imidazole} \quad \text{(i)}$$

$$\text{ISC: MgPc}(S_1)-\text{imidazole} \xrightarrow[\text{ISC}]{28\ \text{ns}} \text{MgPc}(T_1)-\text{imidazole} \xrightarrow{275\ \mu\text{s}} \text{MgPc}-\text{imidazole} \quad \text{(ii)}$$

$$\text{PET: MgPc}(S_1)-\text{imidazole} \xrightarrow[\text{PET}]{26\ \text{ns}} \text{MgPc}^{\bullet-}-\text{imidazole}^{\bullet+} \xrightarrow[\text{CR}]{2\ \text{ns}} \text{MgPc}-\text{imidazole} \quad \text{(iii)}$$

ISC generates T_1 which is 275 μs long-lived and absorbs light in a broad range of wavelength, which may interfere with the observation of other transient species. CSS, however, exhibits a short lifetime of ca. 2 ns due to easy charge recombination (CR), as shown by process iii. By recording spectra in μs scale we can therefore easily identify the transient absorptions of T_1, but not CSS since it is disappeared already.

Fluorescence Studies. The fluorescence emission spectra of MgPc(β-imidazole)$_4$ in DMF were recorded under the same conditions as that of MgPc with excitation at 610 nm. These spectra are compared in Figure 6. Although Φ_f of MgPc(β-imidazole)$_4$ is only 50% of MgPc, decreased to 0.31 from 0.60 of MgPc, the emission spectrum of MgPc(β-imidazole)$_4$ showed very similar shape as that of MgPc, except an 11 nm red shift in emission maximum. This fluorescence quenching is reasonable, because an imidazole unit contains two nitrogen atoms and can act as electron donors, as do histidine residues in peptides or proteins.

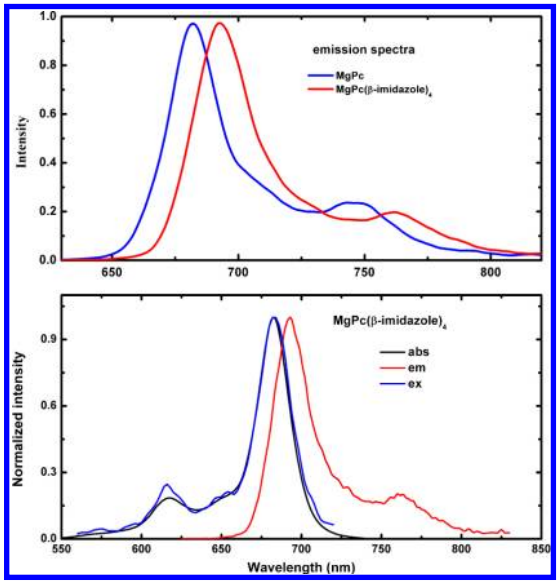

Figure 6. Top: Normalized fluorescence emission spectra with excitation at 610 nm (absorbance 0.090). Bottom: Normalized absorption, fluorescence excitation (emission at 730 nm), and emission spectra (with excitation at 610 nm) for MgPc(β-imidazole)$_4$.

The decay of fluorescence emission at 695 nm is illustrated in Figure 7. A visual examination already tells that the τ_f of MgPc(β-imidazole)$_4$ is shortened with respect to that of MgPc. Both compounds exhibit a typical monoexponential decay with τ_f of 7.49 and 5.85 ns for MgPc and MgPc(β-imidazole)$_4$ respectively. The τ_f shortening is apparently due to PET from imidazole moieties to S_1 of MgPc subunit in the conjugate.

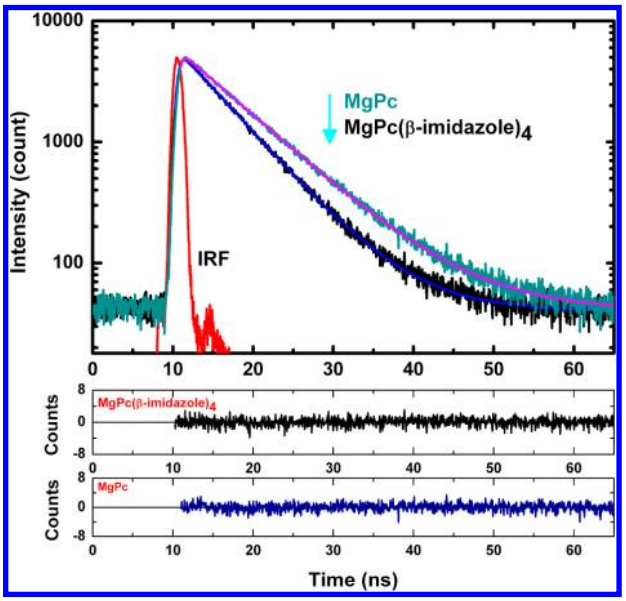

Figure 7. Top: Time profile of fluorescence decay with excitation at 672 nm by a diode laser (50 ps); the emission was monitored at 695 nm, and the concentration of dyes is ca. 2.0 μM. Middle and bottom: fitting residues.

In summary, the fluorescence investigation reveals that PET does occur from imidazole units to the MgPc fragment within the conjugate. With excitation at 610 nm, only the MgPc moiety is populated to S_1, and energy transfer from S_1 of MgPc to imidazole is not allowed, since the emitted photons have much lower energy than that of imidazoles can absorb.

Efficiency and Kinetics of PET. The rate constant of PET (k_{et}) can be calculated from eq 6, in which τ_f^0 is the fluorescence lifetime of MgPc while τ_f is the value for MgPc(β-imidazole)$_4$. k_{et} is thus obtained as 0.37×10^8 s^{-1}.

$$k_{et} = \tau_f^{-1} - (\tau_f^0)^{-1} \quad (6)$$

Efficiency for PET (Φ_{et}) is calculated to be 22% by using the k_{et} value ($\Phi_{et} = k_{et}\tau_f$), which indicates that PET efficiency is comparable to its fluorescence emission ($\Phi_f = 0.31$) in the system. k_f (the rate constant of fluorescence emission from S_1) is 0.53×10^8 s^{-1}, slightly higher than k_{et}.

The summation of Φ_f, Φ_{et}, and Φ_T is 0.79 (= 0.31 + 0.22 + 0.26) for MgPc(β-imidazole)$_4$, close to 0.82 (= $\Phi_f + \Phi_T$ = 0.60 + 0.22) for MgPc. The internal conversion (IC) efficiency of MgPc(β-imidazole)$_4$ can be estimated as 0.21 ($\Phi_{ic} = 1 - \Phi_f - \Phi_T$), slightly higher than 0.18 of MgPc. The substitution of H by imidazole does not significantly enhance IC. The overall processes are shown in Figure 8.

Thermodynamics of PET. The oxidation potential of imidazole was measured to be 0.76 V,[37] while the reduction potential of the phthalocyanine ring is −0.88 V in DMF.[33,38] Electron transfer from imidazole to MgPc ring in their ground states is not thermodynamically allowed, due to the large

dx.doi.org/10.1021/jp3047938 | J. Phys. Chem. A 2012, 116, 7651−7657

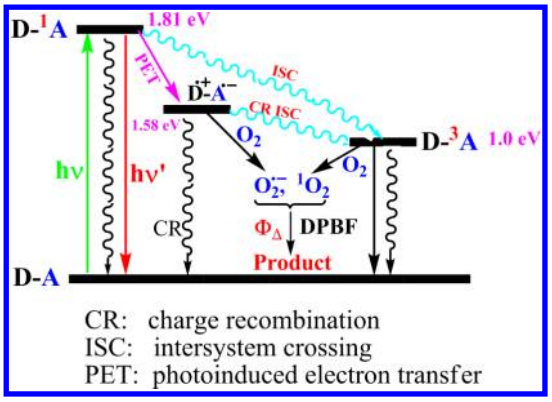

Figure 8. The photophysical and photochemical processes involved in the photooxidation.

positive value of free energy change (ΔG) calculated by $\Delta G_{ET} = E_{ox} - E_{red} - C = 0.76 - (-0.88) - 0.06 = 1.58$ eV, in which E_{ox} is the oxidation potential of a donor, E_{red} represents the reduction potential of an acceptor, and C is a small constant associated with solvent. PET from imidazole to S_1 of MgPc moiety (by the photoexcitation of the Pc moiety), on the other hand, is thermodynamically favored, since its ΔG is a negative value obtained by $\Delta G_{PET} = \Delta G_{ET} - E_{00}$ (MgPc) = 1.58 − 1.81 = −0.23 eV, in which E_{00} is the excitation energy. PET from imidazole donors to T_1 of the MgPc moiety is forbidden, since the energy of the T_1 state is 0.99 eV, which suggests a ΔG of +0.59 eV; this explains why the T_1 state is not quenched by imidazoles.

Singlet Oxygen Formation and DPBF Photooxidation. The quantum yield (Φ_Δ) for photooxidation was measured using the DPBF chemical trapping method with irradiation at 660 nm in air saturated DMF. DPBF degradation was monitored by UV−vis spectra. Figure 9 displays the decrease of [DPBF] upon irradiation time, for which the first order kinetics was observed (inset of Figure 9). Φ_Δ is also included in Table 1. The measured value of Φ_Δ for MgPc(β-imidazole)$_4$ is 0.52, while the maximum quantum yield of singlet oxygen $^1O_2$ ($^1\Delta_g$) production is expected to be the value of Φ_T, i.e., 0.26, since it is generated by energy transfer from T_1 state to molecular oxygen:

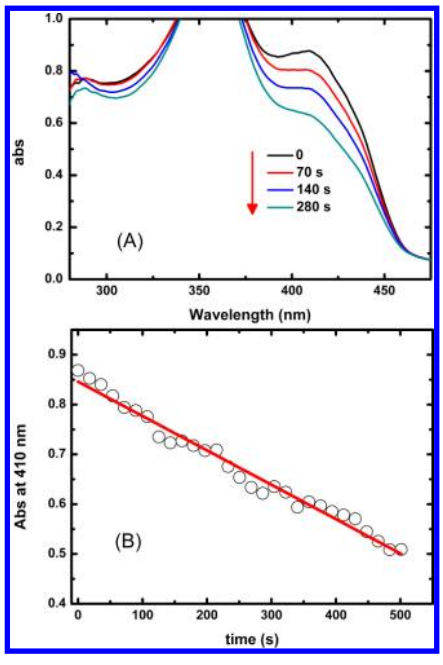

Figure 9. Top: The change of absorption spectrum of 5 μM DPBF upon irradiation time in air saturated DMF containing 11 μM photosensitizer with irradiation at 660 nm. Bottom: The linear plot of absorbance at 415 nm against irradiation time.

$$T_1(PS) + {}^3O_2 \rightarrow S_0(PS) + {}^1O_2({}^1\Delta_g) \quad \text{(iv)}$$

$$DPBF + {}^1O_2({}^1\Delta_g) \rightarrow \text{product type II} \quad \text{(v)}$$

The measured Φ_Δ of 0.52 is significantly greater than the maximum quantum yield of singlet oxygen (0.26). This is due to the fact that DPBF traps not only singlet oxygen but also superoxide anion radical $O_2^{\bullet-}$.[39] Therefore the measured photooxidation efficiency is the sum of two types of oxidations: (1) DPBF oxidized by singlet oxygen and (2) DPBF oxidized by superoxide anion radical $O_2^{\bullet-}$.

For the conjugate, superoxide anion radical $O_2^{\bullet-}$ is produced by the reaction of MgPc$^{\bullet-}$ with molecular oxygen (process vi); this is evidenced by the reaction of oxygen with MgPc$^{\bullet-}$ mentioned previously.

$$MgPc^{\bullet-}\text{−imidazole}^{\bullet+} + O_2 \rightarrow MgPc\text{−imidazole}^{\bullet+} + O_2^{\bullet-} \quad \text{(vi)}$$

$$DPBF + O_2^{\bullet-} \rightarrow \text{product type I} \quad \text{(vii)}$$

The quantum efficiency for CSS generation is 0.22 (Φ_{ET}). In the presence of oxygen the process CR to T_1 is inhibited, such that all CSS is dissipated in process vi, which gives the maximum quantum efficiency of $O_2^{\bullet-}$ generation as 0.22. In this case, all T_1 is originated from S_1 by ISC with the efficiency of 0.26; this is the amount of T_1 that can contribute to the generation of singlet oxygen. Therefore the total efficiency of DPBF photooxidation is expected to be the sum of type II and type I reactions. The summation gave the value 0.48 (= 0.26 + 0.22). This estimated value reasonably agrees with the measured value of 0.52.

We can also roughly estimate the relative importance of type I over type II reaction. The percentage of type I reaction is about 46% (0.22/(0.22 + 0.26)), while the importance of type II reaction is 54%. This result shows that the binding of imidazole can affect the reaction mechanism significantly, while the photo-oxidizing ability of the bioconjugated PS is even increased.

CONCLUSIONS

We have synthesized a bioconjugated PS model compound in which four imidazole units were attached to MgPc through covalent bonding. The photophysical and photochemical processes related to PDT were revealed by comparing the transient and steady state spectra of S_1, T_1, and CSS with that of the free MgPc. PET occurs within the molecule from imidazole subunits to S_1 of the MgPc moiety, which is evidenced by the quenching of Φ_f and τ_f, the presence of transient absorption bands for MgPc$^{\bullet-}$, and the thermodynamic and kinetic analysis. The yield for DPBF photooxidation is much higher than triplet formation yield, due to the good yield of superoxide anion radical generated by the reaction of CSS with oxygen. Type I mechanism accounts for 46% of total reaction. These results suggest that MgPc is still a good PS even

dx.doi.org/10.1021/jp3047938 | J. Phys. Chem. A 2012, 116, 7651−7657

after binding to imidazole units, and the reaction mechanism contains 50% type I contribution.

AUTHOR INFORMATION

Corresponding Author

*E-mail: zhangxianfu@tsinghua.org.cn. Fax: 86 3358357040. Tel: 86 3358357040.

Notes

The authors declare no competing financial interest.

ACKNOWLEDGMENTS

This work has been supported by Hebei Provincial Science Foundation (Contract B2010001518) and HBUST.

REFERENCES

(1) Robertson, C. A.; Evans, D. H.; Abrahamse, H. *J. Photochem. Photobiol., B* **2009**, *96*, 1−8.
(2) Kudinova, N. V.; Berezov, T. T. *Biochem. (Moscow) Suppl. Ser. B: Biomed. Chem.* **2010**, *4*, 95−103.
(3) Plaetzer, K.; Krammer, B.; Berlanda, J.; Berr, F.; Kiesslich, T. *Lasers Med. Sci.* **2009**, *24*, 259−268.
(4) Jiang, X. J.; Yeung, S. L.; Lo, P. C.; Fong, W. P.; Ng, D. K. P. *J. Med. Chem.* **2011**, *54*, 320−330.
(5) Liu, J.-Y.; Lo, P.-C.; Jiang, X.-J.; Fong, W.-P.; Ng, D. K. P. *Dalton Trans.* **2009**, *21*, 4129−4135.
(6) Iqbal, Z.; Masilela, N.; Nyokong, T.; Lyubimtsev, A.; Hanack, M.; Ziegler, T. *Photochem. Photobiol. Sci.* **2012**, *11*, 679−686.
(7) Soldatova, A. V.; Kim, J.; Rizzoli, C.; Kenney, M. E.; Rodgers, M. A. J.; Rosa, A.; Ricciardi, G. *Inorg. Chem.* **2011**, *50*, 1135−1149.
(8) Plaetzer, K.; Krammer, B.; Berlanda, J.; Berr, F.; Kiesslich, T. *Lasers Med. Sci.* **2009**, *24*, 259−268.
(9) Lopez, J. J.; Carter, M. A. G.; Tsentalovich, Y. P.; Morozova, O. B.; Yurkovskaya, A. V.; Hore, P. J. *Photochem. Photobiol.* **2002**, *75*, 6−10.
(10) Zhang, X.-F.; Xu, H.; Shen, T. *Sci. China B* **1995**, *38*, 641−648.
(11) Ferraudi, G.; Arguello, G. A.; Ali, H.; Lier, J. E. *Photochem. Photobiol.* **1988**, *47*, 657−660.
(12) Zhang, X. F.; Xu, H. J. *J. Photochem. Photobiol., B* **1994**, *24*, 109−116.
(13) Segalla, A.; Borsarelli, C. D.; Braslavsky, S. E.; Spikes, J. D.; Roncucci, G.; Dei, D.; Chiti, G.; Jori, G.; Reddi, E. *Photochem. Photobiol. Sci.* **2002**, *1*, 641−648.
(14) Davila, J.; Harriman, A. *Photochem. Photobiol.* **1989**, *50*, 29−35.
(15) Sharman, W. M.; Lier, J. E. v. *Bioconjugate Chem.* **2005**, *16*, 1166−1175.
(16) Valduga, G.; Nonell, S.; Reddi, E.; Jori, G.; Braslavsky, S. E. *Photochem. Photobiol.* **1988**, *48*, 1−5.
(17) Negri, R. M.; Zalts, A.; Román, E. A.; Aramendía, P. F.; Braslavsky, S. E. *Photochem. Photobiol.* **1991**, *53*, 317−322.
(18) Cauchon, N.; Tian, H.; Langlois, R.; La Madeleine, C.; Martin, S.; Ali, H.; Hunting, D.; van Lier, J. E. *Bioconjugate Chem.* **2005**, *16*, 80−89.
(19) Zhang, X. F.; Xu, H. J. *J. Chem. Soc., Faraday Trans.* **1993**, *89*, 3347−3351.
(20) Choi, C. F.; Tsang, P. T.; Huang, J. D.; Chan, E. Y. M.; Ko, W. H.; Fong, W. P.; Ng, D. K. P. *Chem. Commun.* **2004**, *2004*, 2236−2237.
(21) Nyokong, T. *Coord. Chem. Rev.* **2007**, *251*, 1707−1722.
(22) Ogura, S.-i.; Tabata, K.; Fukushima, K.; Kamachi, T.; Okura, I. *J. Porphyrins Phthalocyanines* **2006**, *10*, 1116−1124.
(23) Woehrle, D.; Suvorovab, O.; Gerdesa, R.; Bartelsa, O.; Lapoka, L.; Baziakinab, N.; Makarovb, S.; Slodeka, A. *J. Porphyrins Phthalocyanines* **2004**, *8*, 1020−1041.
(24) Mantareva, V.; Kussovski, V.; Angelov, I.; Borisova, E.; Avramov, L.; Schnurpfeil, G.; Woehrle, D. *Bioorg. Med. Chem.* **2007**, *15*, 4829−4835.
(25) Yusuf, N.; Katiyar, S. K.; Elmets, C. A. *Photochem. Photobiol.* **2008**, *84*, 366−370.
(26) Miller, J. D.; Baron, E. D.; Scull, H.; Hsia, A.; Berlin, J. C.; McCormick, T.; Colussi, V.; Kenney, M. E.; Cooper, K. D. *Toxicol. Appl. Pharmacol.* **2007**, *224*, 290−299.
(27) McKeown, N. B. The Synthesis of Symmetrical Phthalocyanines. In *The Porphyrin Handbook*; Kadish, K. M., Smith, K. M., Guilard, R., Eds.; Academic Press: New York, 2003; Vol. *15*, p 61.
(28) Montalti, M.; Credi, A.; Prodi, L.; Gandolfi, M. T. Photophysical Properties of Organic Compounds. In *Handbook of Photochemistry*, 3rd ed.; Taylor & Francis Group LLC: London, 2006; p 255.
(29) Ishii, K.; Kobayashi, N. The Photophysical Properties of Phthalocyanines and Related Compounds In *The porphyrin handbook*; Kadish, K. M., Smith, K. M., Guilard, R., Eds.; Academic Press: New York, Amsterdam, 2003; Vol. *16*, pp 1−42.
(30) Carmichael, I.; Hug, G. L. *J. Phys. Chem. Ref. Data* **1986**, *15*, 1−250.
(31) Lagorio, M. G.; Dicelio, L. E.; Roman, E. A. S.; Braslavsky., S. E. *J. Photochem. Photobiol., B* **1989**, *3*, 615−624.
(32) Kuznetsova, N.; Gretsova, N.; Kalmykova, E.; Makarova, E.; Dashkevich, S.; Negrimovskii, V.; Kaliya, O.; Luk'yanets, E. *Russ. J. Gen. Chem.* **2000**, *70*, 133−139.
(33) L'her, M.; Pondaven, A. Electrochemistry of Phthalocyanines. In *The Porphyrin Handbook*; Kadish, K. M., Smith, K. M., Guilard, R., Eds.; Academic Press: San Diego, 2003; pp 117−170.
(34) Zhang, X. F.; Xu, H. J.; Chen, D. W. *J. Photochem. Photobiol., B* **1994**, *22*, 235−239.
(35) Zhang, X.-F.; Chang, Y.; Peng, Y.; Zhang, F. *Aust. J. Chem.* **2009**, *62*, 434−440.
(36) Zhang, X. F.; Huang, J.; Zhao, H.; Zheng, X.; Junzhong, Z. *J. Photochem. Photobiol., A* **2010**, *215*, 96−102.
(37) Tugsuz, T. *J. Phys. Chem. B* **2010**, *114*, 17092−17101.
(38) Ough, E.; Nyokong, T.; Creber, K. A. M.; Stillman, M. J. *Inorg. Chem.* **1988**, *27*, 2724−2732.
(39) Ohyashiki, T.; Nunomura, M.; Katoh, T. *Biochim. Biophys. Acta, Biomembr.* **1999**, *1421*, 131−139.